SAR ground moving target estimation and imaging by using Lv's distribution

Yang, Lei; Zhao, Lifan; Wang, Lu; Bi, Guoan

2015

Yang, L., Zhao, L., Wang, L., & Bi, G. (2015). SAR ground moving target estimation and imaging by using Lv's distribution. 2015 16th International Radar Symposium (IRS).

https://hdl.handle.net/10356/82891

https://doi.org/10.1109/IRS.2015.7226293

SAR Ground Moving Target Estimation and Imaging by Using Lv's Distribution

Lei Yang*, Lifan Zhao*, Lu Wang* and Guoan Bi*

*School of Electrical and Electronic Engineering, Nanyang Technological University
50 Nanyang Avenue, School of EEE, Singapore
email: {yanglei, zhao0145, wa0001lu, egbi}@ntu.edu.sg

Abstract: *This paper presents a new SAR ground moving target estimation and imaging algorithm based on a novel Lv's distribution (LVD). LVD is a recently developed time-frequency representation method for multicomponent linear frequency modulated (LFM) signal. Therefore, the proposed algorithm has superior performance in multiple moving target imaging scenario. By using LVD to represent the multiple moving targets in Doppler centroid frequency and chirp rate domain, each targets' Doppler parameters can be easily read, and the target velocities in both slant-range and along-track directions can be estimated accurately. Focused target responses for multiple moving targets can be obtained simultaneously by simply matched-filtering or other advanced approaches. Point target simulations are designed and carried out to validate the effectiveness and superiority of the proposed algorithm.*

1. Introduction

Synthetic aperture radar (SAR) for ground moving target indication (GMTI) and imaging (GMTIm) have been gaining increasing interest in both civilian and military applications [1–5]. In order to enhance the moving target signature, the ground clutter known as the echoes from stationary background should be canceled or suppressed. Commonly, multichannel SAR in along-track configuration is employed [1, 2], and various approaches to filter the moving target signature from the clutter have been devised [3, 4].

SAR is originally designed for imaging of stationary scene. For moving target, its response would be both displaced and smeared. Generally, the target velocity in radial or slant-range will cause the target response displaced, and the target along-track velocity may result in the target response smeared and defocused [1]. To indicate the moving target's true location, a interferometric phase [5] can be retrieved to estimate the target radial velocity for further target geolocation. However, due to the resultant target defocusing, the target signal-to-clutter-noise ratio (SCNR) may degrade even after the clutter suppression. The accuracy of the target motion estimation would be degraded. To achieve a focused target image, matched-filter bank (MFB) is a conventional strategy [1], which requires to build a grid of target motion hypotheses to cover the target truth. However, it would be intractable for multiple moving targets. Time-frequency representation (TFR) [6–8] is introduced to represent the moving targets automatically on a parametric domain, and the target image can be obtained by a simply matched-filter based on the representation. However, the conventional TFR methods [6, 7] can not be recognized as a true representation for the moving target Doppler parameters.

To address the above mentioned issues, in this paper, we adopt an novel Lv's distribution (LVD) [8] to represent the multiple moving targets which are modeled into a multicomponent linear frequency modulated (LFM) signal, in Doppler centroid frequency and chirp rate (CFCR) domain. LVD is capable of representing one of the LFM component as a distinct peak on the CFCR plane, and it is a true

and direct representation for the physical attributes of the moving target LFM signal model [8]. According to the LVD representation, we can simply estimate the moving target velocities in both radial and along-track by numerical calculation. Since the moving targets are represented distinctly by LVD without defocusing, high target's SCNR can be guaranteed in the Doppler CFCR domain. Therefore, high accuracy of moving target estimation can be achieved. Furthermore, due to the accurate representation by LVD, highly focused responses of multiple moving targets can be obtained, simultaneously, by simply matched-filtering (MF) or other advanced approaches [9, 10]. Simulated experiments are designed and carried out to validate the proposed algorithm.

2. SAR-GMTI/GMTIm Signal Model

In this paper, we consider a relatively simple scenario where the target moves with a constant velocity $\mathbf{v}_t$ during a properly selected coherent processing interval (CPI). Consider the moving target trajectory is $\mathbf{r}_t(t_n) = \mathbf{R}_0 + \mathbf{r}_0 + \mathbf{v}_t t_n$, where $\mathbf{R}_0$ is the reference range vector, $\mathbf{r}_0$ is the target location offset from the scene center, and t_n is the slow-time variable within CPI. To accommodate the clutter suppression, multichannel SAR system is employed, where the reference channel is assumed with the flight track $\mathbf{u}_n(t_n) = \mathbf{v}t_n$ and $\mathbf{v}$ denotes the SAR platform velocity. Other channels are generally expressed with the position $\mathbf{u}_n(t_n) + \mathbf{d}_i$, where $\mathbf{d}_i = d_i\vec{\mathbf{x}}$ and d_i is the i-th channel separation from the reference channel and $\vec{\mathbf{x}}$ is the unit vector along the SAR flight track. The radar-to-target range for the reference and i-th channel is

$$||\mathbf{R}_{0t}(t_n)|| = ||\mathbf{r}_t(t_n) - \mathbf{u}_n(t_n)|| \quad \text{and} \quad ||\mathbf{R}_{\mathrm{it}}(\mathrm{t_n})|| = ||\mathbf{r}_{\mathrm{t}}(\mathrm{t_n}) - \mathbf{u}_{\mathrm{n}}(\mathrm{t_n}) - \mathbf{d}_{\mathrm{i}}|| \,, \tag{1}$$

respectively, where $||\cdot||$ denotes the Euclidean norm. Assuming radar pulses with bandwidth B about carrier frequency f_0 are transmitted, the moving target spectra for the reference and i-th channel are

$$S_{0t}(k, t_n) = \exp(-jk\,||\mathbf{R}_{0t}(t_n)||) \quad \text{and} \quad \mathrm{S_{it}(k, t_n)} = \exp(-\mathrm{jk}\,||\mathbf{R}_{\mathrm{it}}(\mathrm{t_n})||) \,, \tag{2}$$

respectively, where $k = 4\pi(f_0+\Delta f)/c$ denotes the wavenumber, $\Delta f \in [-B/2, B/2]$ is the transmitting frequency variation, and c is the speed of light. All the SAR channels travel precisely along the same track but only delayed in time. For moving target, the radar-to-target range will change during the time delay d_i/v ($v = ||\mathbf{v}||$), and we have the radar-to-target range relation as

$$||\mathbf{R}_{it}(t_n - d_i/v)|| \approx ||\mathbf{R}_{0t}(t_n)|| - v_r d_i/v \,. \tag{3}$$

where the range variation is assumed mainly caused by the target radial velocity v_r. The clutter can be simply canceled by subtracting the spectrum of reference channel from that of the time-shifted i-th channel [5], and the moving target spectrum is

$$S(k, t_n) = S_{it}(k, t_n - d_i/v) - S_{0t}(k, t_n) \approx A \cdot S_{0t}(k, t_n) \exp(j\Phi_{\mathrm{In}}/2) \tag{4}$$

where $A = 2j\sin(\Phi_{\mathrm{In}}/2)$ denotes the complex amplitude, $\Phi_{\mathrm{In}} \approx 4\pi v_r d_i/\lambda v$ is the interferometric phase, and λ is the radar wavelength. To access the moving target signatures, $S_{0t}(k, t_n)$ is to be analyzed.

3. SAR Ground Moving Target Estimation and Imaging Algorithm Based on LVD

In (4), we can see the exponential term of $S_{0t}(k, t_n)$, where the range wavenumber k and azimuth slow-time t_n are coupled with each other. This coupling is commonly known as the range migration to be

corrected. Typically, many mature techniques [11, 12] have been introduced for the decoupling or correction of the range migration. After the decoupling, the moving target can be focused in slant-range dimension by range compression, and the range-compressed moving target spectrum can become $s(t_n)$ = $A\exp(-jk_0\,||\mathbf{r}_t(t_n) - \mathbf{u}_n(t_n)|\,|)$ where $k_0 = 4\pi f_0/c = 4\pi/\lambda$ is the wavenumber centroid. Usually, we form a SAR image in slant-range plane. For convenience, we define the following vectors as

$$\mathbf{R}_0 = R_0\vec{\mathbf{r}},\;\; \mathbf{r}_0 = x\vec{\mathbf{x}} + r\vec{\mathbf{r}},\;\; \mathbf{v}_t = v_x\vec{\mathbf{x}} + v_r\vec{\mathbf{r}}, \tag{5}$$

where $\vec{\mathbf{r}}$ represents unit vector of the slant-range, and x and r are the target true locations in azimuth and slant-range dimensions, respectively, and v_x is the along-track component of $\mathbf{v}_t$. By substituting (1), (2) and (5) into $s(t_n)$, and approximating the phase up to second order Taylor series, we can rewrite the range compressed moving target spectrum explicitly as

$$s(t_n) = A\exp[j2\pi f_d t_n + j\pi\gamma_d t_n^2] \tag{6}$$

where $f_d = f_{dc} - f_{dt}$ and $\gamma_d = \gamma_{dc} - \gamma_{dt}$, and

$$f_{dc} = \frac{2v}{\lambda}\frac{x}{R_0},\; f_{dt} = \frac{2v}{\lambda}\frac{(R_0+r)v_r}{R_0},\; \gamma_{dc} = \frac{2}{\lambda}\frac{v^2}{R_0},\; \gamma_{dt} = \frac{2}{\lambda}\frac{(v-v_x)^2 + v_r^2}{R_0}\;. \tag{7}$$

As seen in the derivations of (6) and (7), the moving target signal is modeled as a LFM form. The linear modulated parameter f_d is known as Doppler centroid frequency, and the quadratic modulated parameter γ_d can be referred to Doppler chirp rate. Next, to accommodate multiple moving targets, (6) should be formulated in multicomponent LFM signal as

$$s(t_n) = \sum_{k=1}^{K} A_k\exp[j2\pi f_d^k t_n + j\pi\gamma_d^k t_n^2]\;. \tag{8}$$

3.1. Moving Target Representation by LVD

In this paper, the novel LVD [8] is applied to represent the multiple moving targets in the Doppler CFCR domain. To compute the LVD representation, a parametric symmetric instantaneous autocorrelation function (PSIAF) is defined and calculated as [8]

$$\begin{aligned} R_s^C(\tau, t_n) &= s(t_n + \frac{\tau+a}{2})s^*(t_n - \frac{\tau+a}{2}) \\ &= \sum_{k=1}^{K}\exp[j2\pi f_d^k(\tau+a) + j2\pi\gamma_d^k(\tau+a)t_n] + \sum_{k=1}^{K-1}\sum_{l=k+1}^{K} R_{s_{kl}}^C(\tau, t_n) + R_{s_{lk}}^C(\tau, t_n) \end{aligned} \tag{9}$$

where the superscript * denotes the conjugate operator, τ is the time-lag variable, a is a constant time-delay parameter, and $R_{s_{kl}}^C(\tau, t_n)$ is one of cross-terms of PSIAF. As noted in the exponential terms of (9), which is known as auto-terms, the slow-time variable t_n and time-lag variable τ are coupled with each other. Actually, this coupling is the inherent mechanism causing the degradation of TFR. In our intended problem, this coupling can be interpreted as the migration of Doppler frequency $\gamma_d^k(\tau+a)$ across the slow-time t_n. To remove this coupling or linear Doppler frequency migration, a scaling process in LVD is introduced as [8] $\Gamma[R_s^C(\tau, t_n)]$ = $R_s^C(\tau, \tilde{t}_n/h(\tau+a))$ where $\tilde{t}_n$ is a newly scaled slow-time variable to cope with the scaling process, and h is the scaling factor. Then, the LVD representation is obtained as

$$\mathcal{L}_s(\hat{f}_d, \hat{\gamma}_d) = \mathcal{F}_{\tilde{t}_n}\left\{\mathcal{F}_\tau\left\{\Gamma[R_s^C(\tau, t_n)]\right\}\right\} = \sum_{k=1}^{K}\mathcal{L}_{s_k}(\hat{f}_d, \hat{\gamma}_d) + \sum_{k=1}^{K-1}\sum_{l=k+1}^{K}\mathcal{L}_{s_{kl}}(\hat{f}_d, \hat{\gamma}_d) \tag{10}$$

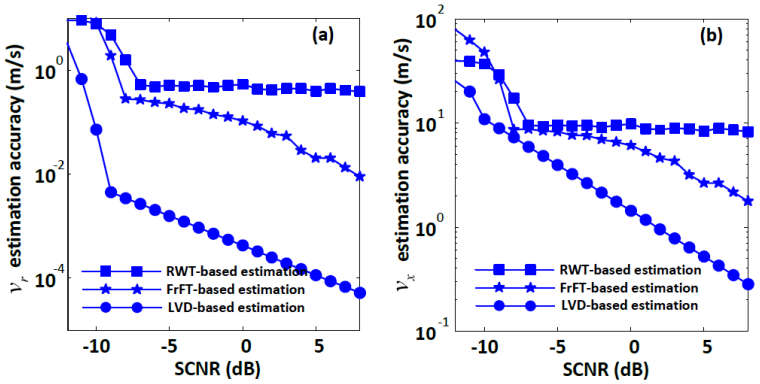

Figure 1: Moving target estimation accuracy.

where $\mathcal{F}_\tau$ and $\mathcal{F}_{\tilde{t}_n}$ are the FT operators with respect to τ and $\tilde{t}_n$, respectively. In (10), $\mathcal{L}_{s_{kl}}(\cdot)$ is one of the cross-terms of the LVD representation. As it has been concluded in [8], LVD maintains asymptotic linearity, and the cross-terms have fairly low amplitude compared with that of auto-terms. According to [8], the two parameters, a and h, are both required to be one for an optimal performance of LVD, and the LVD representation modulus can be given as

$$\left|\mathcal{L}_s(\hat{f}_d, \hat{\gamma}_d)\right| = \sum_{k=1}^{K} \delta(\hat{f}_d - f_d^k)\delta(\hat{\gamma}_d - \gamma_d^k) \tag{11}$$

where $\delta(\cdot)$ is Dirac delta function representing the LVD spread function along the representative axis $\hat{f}_d$ and $\hat{\gamma}_d$. It can be noted from the LVD representation (11) that each moving target modeled in a LFM component is represented in the CFCR domain $(\hat{f}_d, \hat{\gamma}_d)$ by a distinct delta peak with the representative coordinates (f_d^k, γ_d^k).

3.2. Moving Target Estimation and Imaging

According to the LVD representation, the target velocity can be simply calculated as

$$\hat{v}_r^k = \frac{\lambda}{2v}\frac{R_0 + r}{R_0} f_{dt}^k \ , \quad \hat{v}_x^k = v - \sqrt{\frac{\lambda R_0}{2}\gamma_{dt}^k} \ , \tag{12}$$

where f_{dt}^k and γ_{dt}^k are the k-th target Doppler frequency shift and chirp rate difference, and $\hat{v}_r^k$ and $\hat{v}_x^k$ are the k-th target estimations of radial and along-track velocities, respectively. According to [8] ($Theorem$ 5), we give the accuracy of the moving target estimations are bounded as

$$\sigma_{\hat{v}_r}^2 < \frac{\lambda^2(147N^3 + 36q^2N^2)}{4\pi^2(98N^4 + 72q^4)\mathrm{SCNR}_{\mathrm{in}}}, \quad \sigma_{\hat{v}_x}^2 < \frac{\lambda R_0}{2}\sqrt{\frac{294}{\pi^2 N \mathrm{SCNR}_{\mathrm{in}}}} \ , \tag{13}$$

where $\sigma_{\hat{v}_r}^2$ and $\sigma_{\hat{v}_x}^2$ are the variances of the radial and along-track velocity estimations, respectively, and N is the number of sample numbera for the PSIAF, and q equals to $1/F_s$ and F_s is the SAR azimuth sampling frequency or PRF, and $\mathrm{SCNR}_{\mathrm{in}}$ denotes the input SCNR of the target. As noted in (13), both the accuracies are inversely proportional to the input SCNR, which satisfy the practice.

Next, to achieve a focused moving target image, matched-filtering is a simple way according to the LVD representative Doppler chirp rate. Generally speaking, the range-compressed moving target spectrum

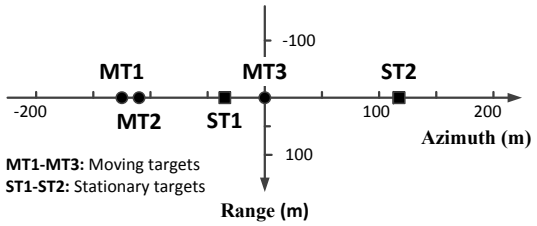

Figure 2: Moving target ground truth.

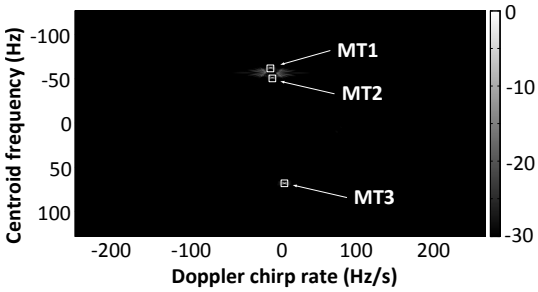

Figure 3: Moving target representation by LVD.

(8) can be rewritten in matrix form as $\mathbf{Y} = \mathbf{AX}$ where $\mathbf{Y}$ is the observation matrix of the range-compressed data. Besides, $\mathbf{A}$ is a polynomial Fourier dictionary with quadratic modulation considered, which is determined under the LVD representation. Besides, $\mathbf{X}$ is the moving target image, which can be obtained by simply matched-filtering as $\mathbf{X} = \mathbf{A}^{-1}\mathbf{Y}$. For more advanced approach, considering additive perturbations $\mathbf{C_n}$, including residual clutter and unavoidable noise, the problem would become $\mathbf{Y} = \mathbf{AX} + \mathbf{C_n}$. Due to the inherent sparsity of moving target image $\mathbf{X}$ in clutter-suppressed SAR image domain, compressive sensing (CS) [9, 10] would be a feasible way for the solution.

4. Experiments

In this section, point target simulations are designed and carried out to validate the proposed SAR ground moving target estimation and imaging algorithm. The SAR sensor is supposed to be an X-band radar with three channels. The SAR platform is assumed flying with a constant velocity 150m/s and the nearest range to the observing scene center is about 10km. CPI is approximately 2s. In total, 3 moving targets are simulated, and each target is simulated with radial and along-track velocities that are randomly selected. Firstly, we analyze the estimation accuracy of the proposed algorithm. In Fig. 1, the estimation accuracy is analyzed with input SCNR from -12dB to 8dB at the step of 1dB. For each input SCNR, RWT [6], FrFT [7] and LVD are used to represent the moving targets, and each method is carried out 10000 trials. Under the representations, the target estimation can be calculated, and the standard variation of the estimation is used to denote the estimation accuracy. From Fig. 1(a) and (b), for both the radial and along-track velocity estimations, we see that the proposed LVD-based estimation has achieved the highest accuracy compared with the other two conventional TFR methods. Secondly, moving target imaging simulation is carried out. Also, 3 moving targets are simulated, and the target ground truth is shown in Fig. 2. Both residual clutter and noise in Gaussian distribution are simulated. As seen from Fig. 2, the 3 moving targets are set to be located closely and within the same range cell. In addition, 2 stationary targets are also simulated in the range cell. By using the LVD to represent the moving targets, the 3 distinct peaks on the Doppler CFCR domain are clearly shown in Fig. 3. Each representative peak's coordinates can be used for further target imaging. In Fig. 4(a), the moving target image is given. Obviously, due to the target movement, the target responses are severely defocused. Especially for MT1 and MT2, which are the two target located closely, their responses are overlapped to each other. Both the target image entropy and target-to-clutter ratio (TCR) are provided to numerically demonstrate the quality of the SAR moving target image. The smaller the image entropy is the better the target focuses, and the higher target TCR is the higher contrast of the image is. Under the LVD representation, the multiple moving targets can be focused simultaneously as shown in Fig. 4(b). However, due to the residual clutter and noise, although the target image is focused in some extent, the image TCR is still not high enough. By using the CS

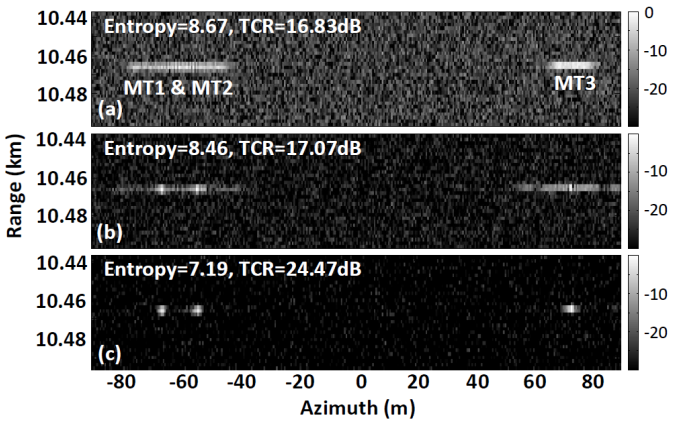

Figure 4: Moving target imaging ((a): defocused moving target image; (b): focused moving target image by MF; (c): focused moving target image by CS;).

framework [9, 10] to solve the imaging problem, in Fig. 4(c), the resultant target image can be improved greatly with better focusing and contrast performance.

References

[1] J. K. Jao, and A. Yegulalp, "Multichannel synthetic aperture radar signatures and imaging of a moving target", *Inverse Problems*, 2013, vol. 29, num. 5, pp. 054009.

[2] G. Sun, M Xing, X. Xia, Y. Wu and Z. Bao, "Robust Ground Moving-Target Imaging Using Deramp?Keystone Processing", *Geoscience and Remote Sensing, IEEE Transactions on*, Feb 2013, vol. 51, no. 2, pp. 966-982.

[3] Wang and H.S.C., "Mainlobe clutter cancellation by DPCA for space-based radars", *Aerospace Applications Conference*, Feb 1991, pp. 1-28.

[4] Guerci and R. Joseph, "Space-time adaptive processing for radar", Artech House, 2003.

[5] Deming, W. Ross, MacIntosh, Scott, and B. Matthew, "Three-channel processing for improved geo-location performance in SAR-based GMTI interferometry", *SPIE Defense, Security, and Sensing*, 2012, pp. 83940F–83940F.

[6] J. C. Wood, and D. T. Barry, "Radon transformation of time-frequency distributions for analysis of multicomponent signals", *Signal Processing, IEEE Transactions on*, Nov 1994, vol. 42, no. 11, pp. 3166-3177.

[7] L. B. Almeida, "The fractional Fourier transform and time-frequency representations", *Signal Processing, IEEE Transactions on*, Nov 1994, vol. 42, no. 11, pp. 3084-3091.

[8] X. Lv, G. Bi, C. Wan, and M. Xing, "Lv's Distribution: Principle, Implementation, Properties, and Performance", *Signal Processing, IEEE Transactions on*, Aug 2011, vol. 59, no. 8, pp. 3576-3591.

[9] L. Zhang, M. Xing, C. Qiu, J. Li, J. Sheng, Y. Li and Z. Bao, "Resolution Enhancement for Inversed Synthetic Aperture Radar Imaging Under Low SNR via Improved Compressive Sensing", *Geoscience and Remote Sensing, IEEE Transactions on*, Oct 2010, vol. 48, no. 10, pp. 3824-3838.

[10] L. Zhao, L. Wang, G. Bi, and L. Yang, "An Autofocus Technique for High-Resolution Inverse Synthetic Aperture Radar Imagery", *Geoscience and Remote Sensing, IEEE Transactions on*, Oct 2014, vol. 52, no. 10, pp. 6392-6403.

[11] L. Yang, M. Xing, Y. Wang, L. Zhang, and Z. Bao, "Compensation for the NsRCM and Phase Error After Polar Format Resampling for Airborne Spotlight SAR Raw Data of High Resolution", *Geoscience and Remote Sensing Letters, IEEE*, Jan 2013, vol. 10, no. 1, pp. 165-169.

[12] M. Soumekh, "Synthetic aperture radar signal processing", Wiley-Interscience, United States of America, 1999.